***JKPK (JURNAL KIMIA DAN PENDIDIKAN KIMIA)**, Vol. 10, No. 2, 2025* *pp. 323-335*
Chemistry Education Study Program, Universitas Sebelas Maret *ISSN 2503-4146*
https://jurnal.uns.ac.id/jkpk *ISSN 2503-4154 (online)*

The Utilization of Zn–C Battery Waste and Duck Eggshells in the Synthesis of ZnO/HAp Composite as a Photocatalyst for Methylene Blue Waste Treatment

Ferli Septi Irwansyah[1*], Nafisah Staustan[2], Eko Prabowo Hadisantoso[1,2], Diana Rakhmawati Eddy[3], and Atiek Rostika Noviyanti[3]

[1]Department of Chemistry Education, UIN Sunan Gunung Djati Bandung, Bandung, Indonesia
[2]Department of Chemistry, UIN Sunan Gunung Djati Bandung, Bandung, Indonesia
[3]Department of Chemistry, Universitas Padjadjaran, Sumedang, Indonesia

ARTICLE INFO

Keywords:
Methylene blue;
photocatalyst;
solid state dispersion;
ZnO/HAp composite.

Article History:
Received: 2025-07-26
Accepted: 2025-08-20
Published: 2025-08-31
doi:10.20961/jkpk.v10i2.106962

©2025 The Authors. This open-access article is distributed under a (CC-BY-SA License)

ABSTRACT

Synthetic dyes such as methylene blue pose a significant pollution threat due to their chemical stability, resistance to biodegradation, and adverse ecological impacts. Photocatalytic treatment with ZnO is promising; however, particle agglomeration commonly diminishes efficiency. To mitigate this limitation, a ZnO/hydroxyapatite (ZnO/HAp) composite was synthesized from Zn–C battery waste and duck eggshells via a solid-state dispersion method using ZnO: HAp molar ratios of 1:1, 1:3, and 3:1. The materials were characterized by X-ray diffraction (XRD) and scanning electron microscopy (SEM). Photocatalytic activity was assessed by degrading 10 mL of 10 ppm methylene blue with 90 mg of photocatalyst under visible-light irradiation for 180 min. XRD confirmed the successful formation of ZnO, HAp, and ZnO/HAp composites with single-phase zincite and hydroxyapatite structures, crystallite sizes of 14.66–25.09 nm, and crystallinity values of 62.66–86.60%. SEM revealed irregular particle morphologies. All composites were photocatalytically active, achieving methylene-blue decolorization of 96.63%, 91.45%, and 81.07%, with the 1:1 composite exhibiting the highest performance. These results indicate that waste-derived ZnO/HAp composites are promising, low-cost photocatalysts for treating organic dye pollutants.

**Corresponding Author*: ferli@uinsgd.ac.id
How to cite: F. S. Irwansyah, N. Staustan, E. P. Hadisantoso, D. R. Eddy, and A. R. Noviyanti, "The Utilization of Zn-C Battery Waste and Duck Eggshells in the Synthesis of ZnO/HAp Composite as a Photocatalyst for Methylene Blue Waste Treatment," *Jurnal Kimia dan Pendidikan Kimia (JKPK)*, vol. 10, no. 2, pp. xx–xx, 2025. [Online]. Available: https://doi.org/10.20961/jkpk.v10i2.106962

INTRODUCTION

In recent decades, rapid industrial growth has become a major contributor to environmental pollution [1], particularly through wastewater containing synthetic dyes from the textile industry [2]. Synthetic dyes exhibit high chemical stability and strong resistance to degradation in conventional wastewater treatment systems. As a result, their accumulation in the environment poses long-term ecological risks [3]. More than 10,000 types of dyes are produced worldwide, with annual production exceeding 7×10^5 tons [2]. Approximately 10–15% of these dyes fail to bind to textile fibers and are ultimately released into the environment [4].

Among them, methylene blue is widely used in the textile industry due to its low cost and high availability [5]. The global

methylene blue market is projected to grow from USD 400 million in 2024 to USD 1 billion by 2037 (CAGR 7.6%), driven by its applications in healthcare, textiles, research, and neurological therapies, along with a growing emphasis on sustainable production [6]. However, methylene blue is toxic, potentially carcinogenic, and harmful to aquatic ecosystems [7], [8]. Therefore, its transformation into more biodegradable and environmentally safe compounds is crucial. Photocatalysis provides an efficient strategy for this purpose. Semiconductor materials such as ZnO, TiO_2, ZrO_2, and Fe_2O_3 are widely recognized as effective photocatalysts capable of degrading methylene blue into simple end-products, including carbon dioxide and water [9].

Zinc oxide (ZnO) is an n-type semiconductor with a 3.37 eV band gap, making it effective under ultraviolet (UV) light for generating electron–hole pairs that drive redox reactions and degrade organic pollutants such as methylene blue [10]. However, its limited response to visible light reduces practical efficiency, as Rabbani et al. (2021) reported that ZnO degraded 41.8% of dye under UV but only 24.9% under visible light [11].

Sustainable synthesis of ZnO from Zn–C battery waste offers ecological and economic benefits by recycling hazardous e-waste and reducing disposal risks [12], [13]. Although zinc from batteries is easily recovered, ZnO suffers from severe agglomeration, which reduces active surface area and charge mobility, thereby lowering photocatalytic performance [14]. Strategies such as doping, surface modification, and composite formation with biowaste-derived materials (e.g., hydroxyapatite from eggshells) have been developed to improve surface area, stability, and activity [15].

Composite development provides a practical solution by preventing agglomeration, enhancing adsorption, and extending ZnO's light absorption into the visible region [16]. Hydroxyapatite (HAp), in particular, is promising in improving dye adsorption and broadening ZnO activity, making ZnO/HAp composites highly attractive for wastewater treatment applications.

Despite the enhanced photocatalytic performance of ZnO/HAp composites, their synthesis from battery waste and eggshell-derived precursors remains underexplored. One promising strategy is the integration of ZnO with porous materials such as HAp [17]. The uniform distribution of ZnO particles on the porous HAp surface increases the active surface area and effectively mitigates particle agglomeration [18].

Recent studies consistently demonstrate that ZnO/HAp composites exhibit superior photocatalytic and antibacterial properties compared to their single-phase counterparts. For instance, hydrothermally synthesized ZnO/HAp composites effectively degraded the antibiotic levofloxacin due to HAp's ability to preconcentrate contaminants around ZnO active sites, thereby enhancing ZnO dispersion and reducing agglomeration [19]. Similarly, ZnO supported on eggshell-derived HAp achieved improved dye removal efficiency. This can be attributed to HAp's high porosity and abundant surface functional

groups (PO_4^{3-}/OH^-), which enhance pollutant adsorption and broaden interfacial contact with ZnO, facilitating light-driven redox reactions [17]. The synergistic interaction arises from HAp acting as an adsorptive matrix that enriches local pollutant concentrations. At the same time, ZnO provides photocatalytic sites for charge separation, resulting in greater stability and overall photocatalytic efficiency [16], [20].

Beyond photocatalysis, HAp is widely utilized for its antibacterial and adsorptive properties, with proven ability to immobilize various organic and inorganic contaminants [18], [21]. HAp can be synthesized from calcium-rich biowaste, including chicken, quail, and duck eggshells [22]. Among these, duck eggshells contain the highest calcium content (77.3%), exceeding that of free-range chicken (52.8%) and quail eggshells (66.13%) as determined by titration of unboiled eggshells [23]. This high calcium content makes duck eggshells an excellent raw material for HAp synthesis with greater yield and purity. Furthermore, valorizing duck eggshell waste reduces its environmental burden—given its slow natural degradation—while providing a low-cost and abundant precursor for sustainable ZnO/HAp composite production.

Several methods have been employed for composite synthesis, including sol–gel [24], [25], hydrothermal [26], [27], and solid-state dispersion techniques [28]. While sol–gel and hydrothermal methods allow precise control over particle size and morphology, they typically require extended processing times, specialized high-pressure equipment, or costly precursors. By contrast, the solid-state dispersion method offers simplicity, low cost, scalability, and environmental compatibility, making it a practical approach for the sustainable preparation of ZnO/HAp composites [28].

This study synthesized ZnO from zinc–carbon battery waste via the coprecipitation method, while HAp was obtained from duck eggshells through a hydrothermal process. The ZnO/HAp composites were subsequently prepared using the solid-state dispersion method and tested for their photocatalytic activity in degrading methylene blue. This approach addresses waste management challenges by transforming hazardous battery residues and eggshell byproducts into functional materials and advancing sustainable photocatalyst development. ZnO provides strong photocatalytic activity, whereas HAp contributes porosity and phosphate groups that enhance pollutant adsorption and charge separation, improving stability and efficiency. The novelty of this work lies in the dual valorization of waste materials through a simple, low-cost, and eco-friendly synthesis route. It is hypothesized that the resulting ZnO/HAp composite exhibits enhanced photocatalytic activity under visible light, offering sustainable potential for wastewater treatment applications.

METHODS

1. Materials

The materials used in this study included zinc–carbon (Zn–C) battery waste and duck eggshells as precursor sources. The chemical reagents comprised hydrochloric acid (HCl, 37%, Merck®),

sodium hydroxide (NaOH, p.a., Merck®), silver nitrate ($AgNO_3$, p.a., Merck®), diammonium hydrogen phosphate ($(NH_4)_2HPO_4$, technical grade), ammonium hydroxide (NH_4OH, 25%, technical grade), and tartaric acid (technical grade). All chemicals were used as received, without further purification.

2. Synthesis of ZnO from Battery Waste

Zinc plates in the second layer of Zn–C battery cells were separated and mechanically cleaned from adhering impurities, particularly carbon paste, by sanding. The cleaned plates were cut into small pieces (~1 × 1 mm). A total of 0.78 g of zinc was dissolved in 100 mL of 5 M HCl under constant stirring until complete dissolution, producing $ZnCl_2$ solution. The pH of the solution was then adjusted to 10 by dropwise addition of 5 M NaOH, resulting in the precipitation of Zn^{2+} ions as $Zn(OH)_2$.

The precipitate was filtered using Whatman No. 41 filter paper, washed repeatedly with distilled water until a neutral pH was achieved, and dried in an oven at 110°C for 3 hours. The dried $Zn(OH)_2$ was subsequently calcined at 400°C for three hours in a muffle furnace (Thermo FB1410 M33, 1100°C) to obtain ZnO powder. The resulting ZnO was characterized by X-ray diffraction (XRD) to confirm its crystalline phase and structural properties.

3. Synthesis of Hydroxyapatite (HAp)

Duck eggshells were cleaned under running tap water, separated from the membranes, oven-dried, and crushed into fine powder. The powdered shells were calcined at 1000°C for 12 h, converting calcium carbonate ($CaCO_3$) into calcium oxide (CaO) [18].

For HAp synthesis, 11.2 g of CaO was dispersed in 150 mL of deionized water containing 1 wt% tartaric acid as a morphology-regulating template [29]. Subsequently, 15.85 g of $(NH_4)_2HPO_4$ was added, and the mixture was stirred until homogeneous. The pH was adjusted to 10 using 25% NH_4OH. The resulting suspension was transferred into a 150 mL Teflon-lined stainless steel autoclave and subjected to hydrothermal treatment at 175°C for eight hours.

After cooling, the precipitate was filtered, washed with deionized water until neutral pH, and dried at 105°C for 24 h. The dried powder was then calcined at 500°C for 3 h to improve crystallinity. XRD confirmed phase purity and crystallinity of Hap.

4. Synthesis of ZnO/HAp Composite

ZnO and HAp powders were mixed in molar ratios of 1:1 (Kom-11), 1:3 (Kom-13), and 3:1 (Kom-31). Each mixture was dispersed in acetone and ultrasonicated for 30 min at room temperature using a GT Sonic UC3LD (220–240 V, 50 Hz, 3 A fuse) to achieve uniform distribution. After solvent evaporation under ambient conditions, the dried solids were calcined at 400°C for three hours. XRD characterized the composites to determine crystallinity and used scanning electron microscopy (SEM) to observe morphology.

5. Photocatalytic Activity Performance

Photocatalytic activity was evaluated using methylene blue (MB) as a model dye

pollutant. A total of 90 mg of ZnO/HAp composite was added to 10 mL of 10 ppm MB solution in a glass vial. The suspension was irradiated with visible light from a 500 W Philips lamp (wavelength range: 400–750 nm, distance: 15 cm) for 180 min. After irradiation, the suspension was filtered to separate the photocatalyst, and the absorbance of the filtrate was measured at 664 nm using a UV–Vis spectrophotometer to determine the decolorization efficiency.

RESULT AND DISCUSSION

1. Structural Characterization (XRD)

X-ray diffraction (XRD) analysis was performed to determine the crystal structures of the synthesized ZnO, HAp, and ZnO/HAp composites. As shown in Figure 1, the diffraction patterns of all samples corresponded well with standard reference patterns. For ZnO, distinct diffraction peaks were observed at 2θ values of approximately 31.77°, 34.42°, 36.25°, 47.53°, and 56.60°, corresponding to the lattice planes (100), (002), (101), (102), and (110), respectively. These peaks are in agreement with the ICDD card number. 00-036-1451, as reported in previous studies [30], [31]. The sharp and intense peaks confirm the formation of the zincite phase, which crystallizes in a hexagonal structure with space group $P6_3mc$.

In the case of hydroxyapatite (HAp), characteristic peaks were observed at 2θ values of 25.88°, 28.92°, 31.76°, 32.89°, 39.79°, 42.32°, 46.69°, 49.49°, 53.22°, and 64.14°, corresponding to the lattice planes (002), (210), (211), (300), (130), (302), (222), (213), (004), and (323), respectively. These results are consistent with the ICDD card number. 01-074-0566 and confirm the formation of a hydroxyapatite phase with a hexagonal structure (space group $P6_3/m$), in line with earlier reports [32]. Although minor variations in peak intensity and slight shifts to lower and higher angles were observed compared with the standards, the coexistence of these characteristic peaks in the composites indicates the successful integration of ZnO and Hap.

Crystallite size and degree of crystallinity were further calculated using the Debye–Scherrer equation, with FWHM data processed through Origin software. The results are summarized in Table 1. The crystallite sizes of all synthesized samples fall within the nanocrystalline range (1–100 nm), confirming that the synthesis produced nanostructured materials. Such nanoscale crystallinity is advantageous for photocatalytic applications, as it typically enhances surface reactivity and increases active surface area.

The results show that pure ZnO exhibited the largest crystallite size and the highest crystallinity, indicating a well-ordered crystalline phase with minimal lattice defects. In contrast, HAp displayed smaller crystallite sizes and lower crystallinity, suggesting the presence of partially amorphous regions likely formed during synthesis.

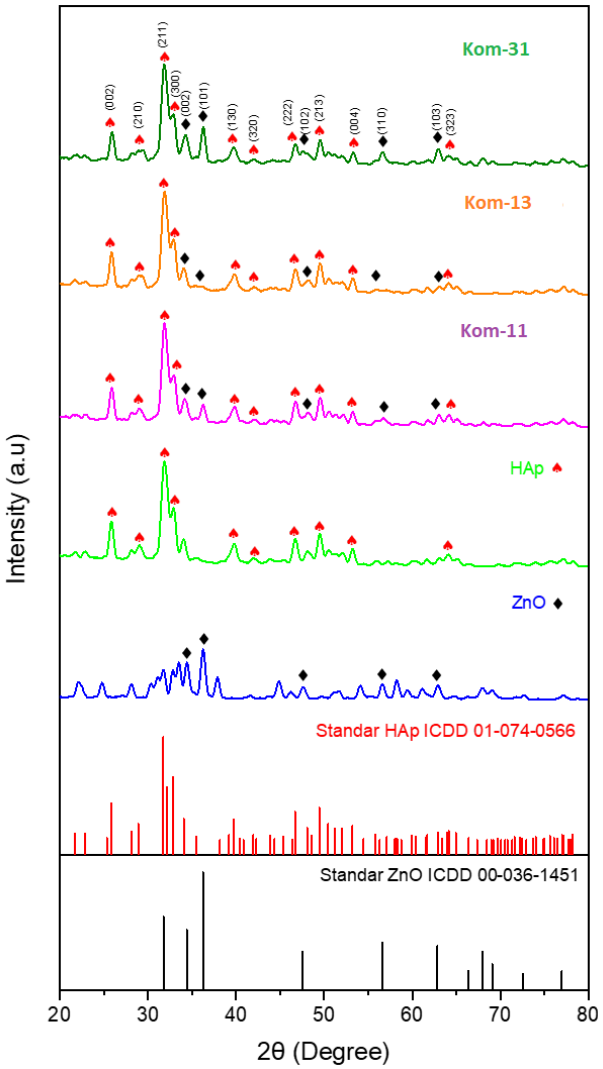


Figure 1. XRD Difractograms

Table 1. Crystallite Size and Degree of Crystallinity

No	Sample	Crystallite Size (nm)	Degree of Crystallinity (%)
1	ZnO	25.10	86.60
2	HAp	16.31	62.66
3	Kom-11	14.67	84.52
4	Kom-13	16.20	66.22
5	Kom-31	18.71	64.03

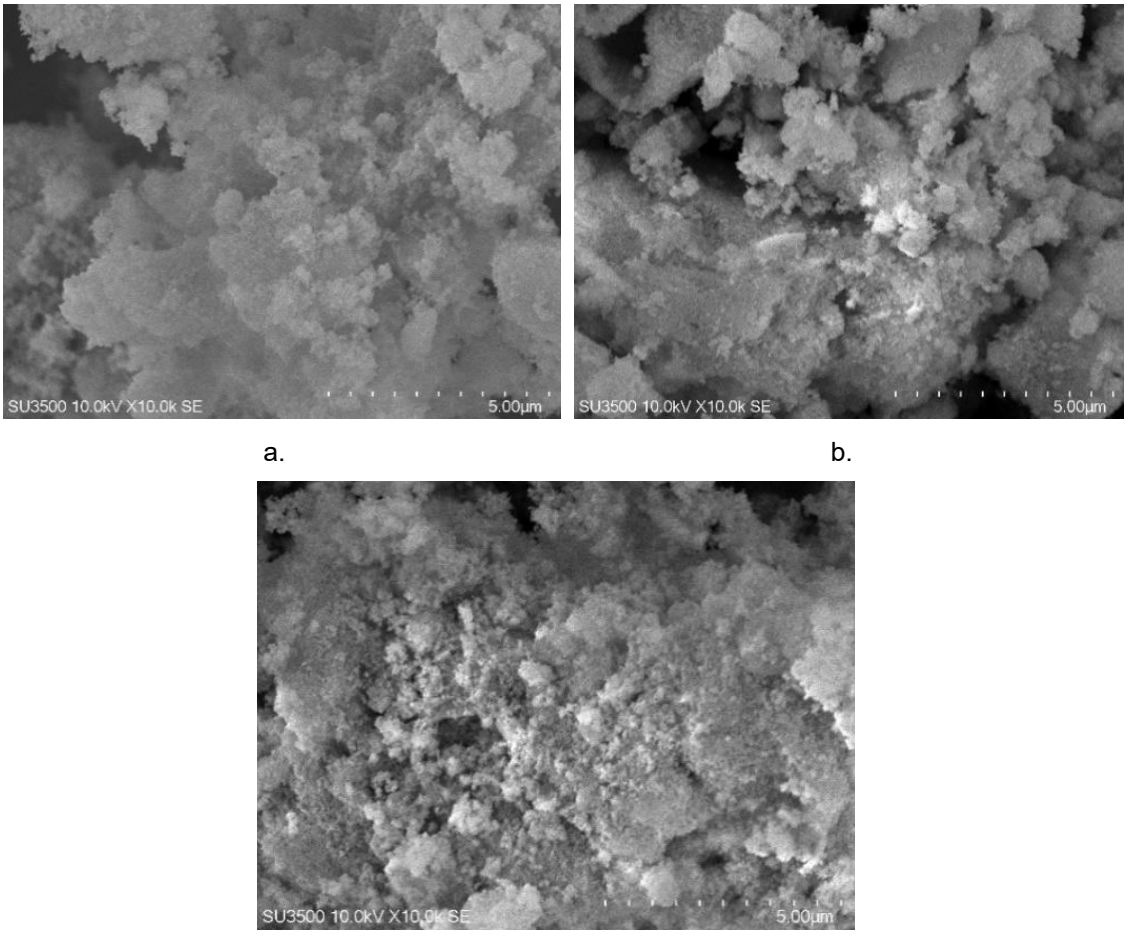
When ZnO and HAp were combined, notable changes in crystallite properties were observed. The composite with a ZnO: HAp ratio of 1:1 (Kom-11) exhibited the smallest crystallite size alongside relatively high crystallinity compared with other composites. This indicates that a balanced composition of ZnO and HAp can suppress excessive crystal growth while maintaining structural consistency. The synergistic interaction between ZnO and HAp stabilizes the

composite structure and optimizes surface characteristics.

Overall, the Kom-11 composite demonstrated the most favorable characteristics—small crystallite size and sufficient crystallinity—expected to enhance its photocatalytic performance. These findings highlight that tailoring the ZnO: HAp ratio is a promising strategy for designing efficient photocatalysts with improved stability and reactivity.

2. Morphology Analysis (SEM)

The surface morphology of the ZnO/HAp composites was analyzed using scanning electron microscopy (SEM). Figure 2 presents the SEM micrographs of the three composites (Kom-11, Kom-13, and Kom-31) at 10,000× magnification. The images reveal that all composites exhibit irregular particle shapes with rough and uneven surfaces, accompanied by noticeable particle aggregation. In addition, variations in particle size suggest a relatively broad size distribution across the samples.



a. b.

c.

Figure 2. SEM Image (a) Kom-11, (b) Kom-13, dan (c) Kom-31, with 10.000x magnification

Among the three composites, Kom-11 displays smaller and more uniformly distributed particles than Kom-13 and Kom-31. Although aggregation is still evident, the overall distribution of particles appears more homogeneous. These results are consistent

with the XRD findings, which showed that Kom-11 possessed the smallest crystallite size, relatively high crystallinity, and a more stable structure. Such features are advantageous because they increase the available surface area, enhancing the potential for catalytic activity [33], [34].

In contrast, Kom-13 and Kom-31 show larger particle aggregates and less uniform size distribution. The rough surface texture and high degree of agglomeration in these samples may hinder the accessibility of active sites on the composite surface, potentially reducing photocatalytic efficiency.

The combined evidence from XRD and SEM indicates that Kom-11 exhibits the most favorable morphological characteristics for photocatalytic applications. Its smaller particle size and relatively homogeneous distribution provide a larger effective contact area for interactions with pollutant molecules, which is expected to enhance photocatalytic degradation efficiency [35].

3. Photocatalytic Performance

The photocatalytic activity of ZnO, HAp, and the ZnO/HAp composites was evaluated through methylene blue (MB) degradation under visible-light irradiation. Figure 3 illustrates the photodegradation performance, showing the number of degraded moles and decolorization percentage. The composites exhibited higher photocatalytic efficiency than the individual components, confirming the synergistic interaction between ZnO and HAp. ZnO primarily serves as a photocatalyst by generating reactive oxygen species, whereas HAp contributes by providing adsorption sites, enhancing ZnO dispersion, and limiting particle agglomeration [36], [37].

Table 2. Data of Photocatalytic Performance

Sample	Initial abs	Final abs	% decolorization	Mol degraded
ZnO	1.9185	0.6277	67.37	19.42
HAp	1.791	0.4335	75.91	20.42
Kom-11	1.9805	0.0692	96.63	28.76
Kom-13	1.9185	0.1664	91.45	26.36
Kom-31	1.9185	0.3653	81.07	23.37

Practically, the number of moles degraded reflects the absolute quantity of decomposed pollutant, while the decolorization percentage indicates overall degradation efficiency, i.e., the fraction of the dye removed. These results are consistent with previous reports showing that ZnO/HAp composites exhibit higher photocatalytic activity than their individual components, primarily because ZnO particles are more evenly dispersed within the HAp matrix, thereby expanding the active surface area and facilitating charge separation and catalyst reusability [30].

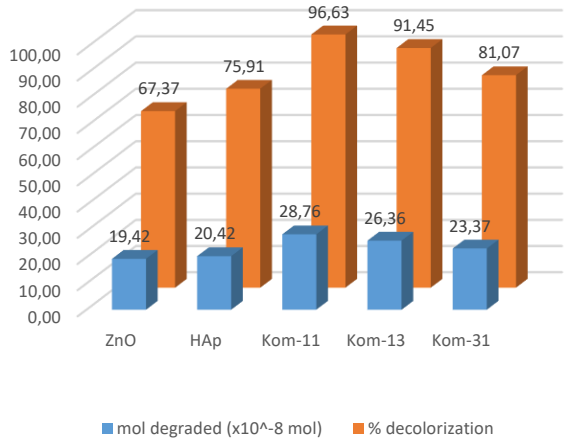


Figure 3. The photocatalytic degradation of methylene blue.

The synergistic interaction between ZnO and HAp explains the observed improvement. Pure ZnO and HAp showed relatively low activity, with decolorization efficiencies of 67.37% and 75.91%, respectively, whereas the composites demonstrated substantially higher performance. Kom-11, with a 1:1 molar ratio, exhibited the best result, achieving 96.63% decolorization, indicating that nearly all methylene blue molecules were degraded under photocatalytic conditions.

At this balanced ratio, ZnO's photocatalytic function and HAp's adsorptive capacity complement each other, enabling more efficient adsorption of dye molecules onto the composite surface, followed by rapid degradation at ZnO active sites. Additionally, HAp increases the local concentration of pollutants near ZnO and enhances ZnO particle dispersion, reducing agglomeration and improving surface accessibility. Crystallite size also plays a significant role: smaller crystallites provide larger specific surface areas and more active sites for redox reactions [38]. XRD results confirmed that Kom-11 had the smallest crystallite size, while SEM analysis revealed a more homogeneous particle distribution, both supporting its superior photocatalytic activity.

Overall, the correlation between crystallite size, surface morphology, and degradation efficiency confirms that ZnO/HAp composites—particularly at the 1:1 molar ratio—offer an effective and sustainable approach for enhancing photocatalytic efficiency in wastewater treatment applications.

CONCLUSION

ZnO, HAp, and ZnO/HAp composites were successfully synthesized from zinc–carbon battery waste and duck eggshells. XRD analysis confirmed the formation of single-crystalline zincite and hydroxyapatite phases with crystallite sizes ranging from 14.66 to 25.09 nm and crystallinity levels between 62.66% and 86.60%. SEM

observations revealed irregular morphologies with varying particle sizes. All ZnO/HAp composites exhibited significant photocatalytic activity toward methylene blue degradation, achieving decolorization efficiencies of 96.63%, 91.45%, and 81.07%, respectively. Among them, the composite with a 1:1 ZnO: HAp ratio (Kom-11) demonstrated the highest performance, attributed to its smaller crystallite size, enhanced surface area, and improved ZnO dispersion within the HAp matrix. These findings highlight the potential of ZnO/HAp composites derived from biowaste as sustainable photocatalysts for wastewater treatment applications.

ACKNOWLEDGEMENT

The authors express their gratitude to UIN Sunan Gunung Djati Bandung for providing the necessary facilities and to LITABDIMAS for providing the funding for this research (B-197.A/Un.05/V.2/HK.00.6/06/2025).

REFERENCES

[1] Iftkhar, A. Md, A. Aftab, A. Fatima, *et al.*, “A comprehensive review on the advancement of transition metals incorporated on functional magnetic nanocomposites for the catalytic reduction and photocatalytic degradation of organic pollutants,” *Coord. Chem. Rev.*, vol. 514, 2024, doi: 10.1016/j.ccr.2024.215904.

[2] A.P. Sahu and J. C. Poler, “Removal and degradation of dyes from textile industry wastewater: Benchmarking recent advancements, toxicity assessment and cost analysis of treatment processes,” *J. Environ. Chem. Eng.*, vol. 12, no. 5, pp. 2213–3437, 2024, doi: 10.1016/j.jece.2024.113754.

[3] R. Al-Tohamy *et al.*, “A critical review on the treatment of dye-containing wastewater: Ecotoxicological and health concerns of textile dyes and possible remediation approaches for environmental safety,” *Ecotoxicol. Environ. Saf.*, vol. 231, 2022, doi: 10.1016/j.ecoenv.2021.113160.

[4] H. S. Rai, M. S. Bhattacharyya, J. Singh, T. K. Bansal, P. Vats, and U. C. Banerjee, “Removal of dyes from the effluent of textile and dyestuff manufacturing industry: A review of emerging techniques with reference to biological treatment,” *Crit. Rev. Environ. Sci. Technol.*, vol. 35, no. 3, pp. 219–238, 2005, doi: 10.1080/10643380590917932.

[5] R. H. Waghchaure, V. A. Adole, and B. S. Jagdale, “Photocatalytic degradation of methylene blue, rhodamine B, methyl orange, and Eriochrome black T dyes by modified ZnO nanocatalysts: A concise review,” *Inorg. Chem. Commun.*, vol. 143, 2022,doi:10.1016/j.inoche.2022.109764.

[6] “Methylene blue market size & share, by application (aquaculture, healthcare, laboratory research, and textile dyeing); form; grade; distribution channel; and purity - Global supply & demand analysis, growth forecasts, statistics report 2025–2037.”

[7] C. Zaharia, D. Suteu, A. Muresan, R. Muresan, and A. Popescu, “Textile wastewater treatment by homogeneous oxidation with hydrogen peroxide,” *Environ. Eng. Manag. J.*, vol. 8, no. 6, pp. 1359–1369, 2009, doi: 10.30638/eemj.2009.199.

[8] S. Sudarshan *et al.*, “Impact of textile dyes on human health and bioremediation of textile industry

effluent using microorganisms: Current status and future prospects," *J. Appl. Microbiol.*, vol. 134, no. 2, pp. 1–23, 2023, doi: 10.1093/jambio/lxac064

[9] S. Goktas and A. Goktas, "A comparative study on recent progress in efficient ZnO based nanocomposite and heterojunction photocatalysts: A review," *J. Alloys Compd.*, vol. 404–406, no. Spec. Iss., pp. 2–22, 2021, doi: 10.1016/j.jallcom.2005.05.002.

[10] A.R. Bhapkar and S. Bhame, "A review on ZnO and its modifications for photocatalytic degradation of prominent textile effluents: Synthesis, mechanisms, and future directions," *J. Environ. Chem. Eng.*, vol. 12, no. 3, 2024,doi: 10.1016/j.jece.2024.112553.

[11] M. Rabbani, J. Shokraiyan, R. Rahimi, and R. Amrollahi, "Comparison of photocatalytic activity of ZnO, Ag-ZnO, Cu-ZnO, Ag, Cu-ZnO and TPPS/ZnO for the degradation of methylene blue under UV and visible light irradiation," *Water Sci. Technol.*, vol. 84, no. 7, pp. 1813–1825, 2021, doi: 10.2166/wst.2021.360.

[12] R. Farzana, R. Rajarao, P. R. Behera, K. Hassan, and V. Sahajwalla, "Zinc oxide nanoparticles from waste Zn-C battery via thermal route: Characterization and properties," *Nanomaterials*, vol. 8, no. 9, 2018, doi: 10.3390/nano8090717.

[13] R. Farzana, R. Rajarao, P. R. Behera, K. Hassan, and V. Sahajwalla, "Zinc oxide nanoparticles from waste Zn-C battery via thermal route: Characterization and properties," *Nanomaterials*, vol. 8, no. 9, 2019, doi: 10.3390/nano8090717.

[14] E. Hadisantoso, P. Listiani, and S. Setiadji, "Preparation of ZnO/SiO2 composite from battery waste and rice husk ash for decolorization of methylene blue," 2020, doi: 10.4108/eai.11-7-2019.2297521.

[15] C. El Bekkali *et al.*, "Zinc oxide-hydroxyapatite nanocomposite photocatalysts for the degradation of ciprofloxacin and ofloxacin antibiotics," *Colloids Surf. A Physicochem. Eng. Asp.*, 2017. doi: 10.1016/j.colsurfa.2017.12.051

[16] K. Tanji *et al.*, "Fast photodegradation of rhodamine B and caffeine using ZnO-hydroxyapatite composites under UV-light illumination," *Catal. Today*, vol. 388–389, pp. 176–186, 2022, doi: 10.1016/j.cattod.2020.07.044.

[17] Y. Chen, R. Zou, and Q. Wu, "Facile synthesis of hollow ZnO/HAp microsphere photocatalysts for efficient removal of tetracycline under full light irradiation," *Inorg. Chem. Commun.*, vol. 174, 2025, doi: 10.1016/j.inoche.2025.114084.

[18] F. S. Irwansyah *et al.*, "How to make and characterize hydroxyapatite from eggshell using the hydrothermal method: Potential insights for drug delivery system," *Indones. J. Sci. Technol.*, vol. 8, no. 3, pp. 469–486, 2023, doi: 10.17509/ijost.v8i3.60825.

[19] A.D. Go, F. D. M. dela Rosa, D. H. Camacho, and E. R. Punzalan, "Photocatalytic degradation of levofloxacin using ZnO/hydroxyapatite nanocomposite: Optimization using response surface methodology," *Chem. Data Collect.*, vol. 50, 2024, doi: 10.1016/j.cdc.2024.101126.

[20] R. K. Dewi *et al.*, "Synthesis and morphological investigation of hydroxyapatite/zinc oxide and evaluation of its application in removal of organic pollutants," *J. Nanostructures*, vol. 11, no. 2, pp. 368–376, 2021, doi: 10.22052/JNS.2021.02.016.

[21] F. S. Irwansyah, A. I. Amal, and E. P. Hadisantoso, "How to make and characterize hydroxyapatite from eggshell using the hydrothermal method: Potential insights for drug delivery system," *Indones. J. Sci. Technol.*, vol. 8, no. 3, pp. 469–486, 2023. doi: 10.17509/ijost.v8i3.60825

[22] A.R. Noviyanti *et al.*, "A novel hydrothermal synthesis of nanohydroxyapatite from eggshell-calcium-oxide precursors," *Heliyon*, vol. 6, no. 4, 2020, doi: 10.1016/j.heliyon.2020.e03655.

[23] M. Y. Azis, T. R. Putri, F. R. Aprilia, Y. Ayuliasari, O. A. D. Hartini, and M. R. Putra, "Eksplorasi kadar kalsium (Ca) dalam limbah cangkang kulit telur bebek dan burung puyuh menggunakan metode titrasi dan AAS," *al-Kimiya*, vol. 5, no. 2, pp. 74–77, 2019, doi: 10.15575/ak.v5i2.3834.

[24] M. Safari Gezaz, S. Mohammadi Aref, and M. Khatamian, "Investigation of structural properties of hydroxyapatite/zinc oxide nanocomposites: An alternative candidate for replacement in recovery of bones in load-tolerating areas," *Mater. Chem. Phys.*, vol. 226, pp. 169–176, 2019, doi:10.1016/j.matchemphys.2019.01.005.

[25] K. Davis, R. Yarbrough, M. Froeschle, J. White, and H. Rathnayake, "Band gap engineered zinc oxide nanostructures via a sol-gel synthesis of solvent driven shape-controlled crystal growth," *RSC Adv.*, vol. 9, no. 26, pp. 14638–14648, 2019, doi: 10.1039/c9ra02091h.

[26] B. Ben Salem *et al.*, "Synthesis and comparative study of the structural and optical properties of binary ZnO-based composites for environmental applications," *RSC Adv.*, vol. 13, no. 9, pp. 6287–6303, 2023, doi: 10.1039/d2ra07837f.

[27] K. P. Sharma, M. Shin, G. P. Awasthi, S. Cho, and C. Yu, "One-step hydrothermal synthesis of CuS/MoS2 composite for use as an electrochemical non-enzymatic glucose sensor," *Heliyon*, vol. 10, no. 2, p. e23721, 2024, doi: 10.1016/j.heliyon.2023.e23721.

[28] R. Munir *et al.*, "The solid state dispersion method for synthesizing eggshells ES/TiO2 composite to enhance photocatalytic degradation methylene blue," *MethodsX*, vol. 14, 2025,doi: 10.1016/j.mex.2024.103150.

[29] A.I. Bucur, R. A. Bucur, Z. Szabadai, C. Mosoarca, and P. A. Linul, "Influence of small concentration addition of tartaric acid on the 220 °C hydrothermal synthesis of hydroxyapatite," *Mater. Charact.*, vol. 132, pp. 76–82, 2017, doi: 10.1016/j.matchar.2017.07.047.

[30] M. S. Elsayed, I. A. Ahmed, D. M. D. Bader, and A. F. Hassan, "Green synthesis of nano zinc oxide/nanohydroxyapatite composites using date palm pits extract and eggshells: Adsorption and photocatalytic degradation of methylene blue," *Nanomaterials*, vol. 12, no. 1, 2022, doi: 10.3390/nano12010049

[31] R. M. Mohamed and E. Aazam, "Synthesis and characterization of Pt-ZnO-hydroxyapatite nanoparticles for photocatalytic degradation of benzene under visible light," *Desalin. Water Treat.*, vol. 51, no. 31–33, pp. 6082–6090, 2013, doi: 10.1080/19443994.2013.764488.

[32] Charlena, I. H. Suparto, and E. Kurniawan, "Synthesis and characterization of hydroxyapatite-zinc oxide (HAp-ZnO) as antibacterial

biomaterial," *IOP Conf. Ser. Mater. Sci. Eng.*, vol. 599, 2019, doi:10.1088/1757899X/599/1/012011.

[33] Y. M. Pusparizkita, R. A. Faizal, S. A. Perwira, R. Ismail, J. Jamari, and A. P. Bayuseno, "A microwave-assisted hydrothermal method for rapidly synthesizing nanocrystalline carbonated hydroxyapatite from calcium resources in crab shell waste," *Next Mater.*, vol. 9, no. 3, p. 100946, 2025,doi:10.1016/j.nxmate.2025.100946.

[34] S. Hossain, "Crystalline structure modification of hydroxyapatite via a hydrothermal method," *Mater. Adv.*, pp. 3889–3902, 2025, doi: 10.1039/d5ma00334b.

[35] W. Nabgan *et al.*, "A review on the design of nanostructure-based materials for photoelectrochemical hydrogen generation from wastewater: Bibliometric analysis, mechanisms, prospective, and challenges," *Int. J. Hydrogen Energy*, vol. 52, pp. 622–663, 2023, doi: 10.1016/j.ijhydene.2023.05.152.

[36] B. E. Nagay, S. S. Malheiros, M. H. R. Borges, C. Aparicio, J. J. J. P. Van Den Beucken, and V. A. R. Bar, "Progress in visible-light-activated photocatalytic coatings to combat implant-related infections: From mechanistic to translational roadmap," *Bioact. Mater.*, vol. 51, pp. 83–137, 2025, doi: 10.1016/j.bioactmat.2025.04.037.

[37] R. Wu, Y. Wang, J. Wang, G. Tian, Y. Li, and C. Liu, "Facile preparation of Fe3O4/HAp/Ag nanomaterial and photocatalytic degradation of four types of dyes with mechanism," *RSC Adv.*, pp. 27128–27138, 2025, doi: 10.1039/d5ra03777h.

[38] C. Mita *et al.*, "High stability and photocatalytic activity of N-doped ZrO2 thin films," *J. Alloys Compd.*, vol. 1002, p. 175134, 2024, doi: 10.1016/j.jallcom.2024.175134.